Journal of Energy Storage 51 (2022) 104471

Contents lists available at ScienceDirect

Journal of Energy Storage

journal homepage: www.elsevier.com/locate/est

Research Papers

Simulation of galvanostatic charge-discharge curves of carbon-based symmetrical electrochemical supercapacitor with organic electrolyte employing potential dependent capacitance and time domain analytical expressions

A.P.R. Fernandez [*], E.A. Périgo [1], R.N. Faria

Nuclear and Energy Research Institute, Sao Paulo 05508-000, Brazil

ARTICLE INFO

Keywords:
Supercapacitors
electrical potential dependent capacitance
time domain analysis
galvanostatic cycle and simulation of galvanostatic curves

ABSTRACT

Electrochemical supercapacitors differ from conventional supercapacitors mainly because they have a very high storage of electrical energy per unit of mass and a capacitance dependent on electrical potential. When studying electrical circuits in the time domain that aim to simulate the curves generated in the charging and discharging processes of electrochemical supercapacitors, as is the case with galvanostatic curves, the capacitance dependent on the electrical potential becomes a factor that considerably increases the degree of difficulty in obtaining the equations for simulating such curves. In this paper, a straightforward electrical circuit was used and fed by a source of electric current I of constant intensity in time in order to simulate the galvanostatic curve properties of a symmetrical supercapacitor evaluated by a galvanostatic cycle technique. Simulation of galvanostatic curves of these carbon-based supercapacitors with organic electrolyte also considered the effects of capacitance dependent on electric potential and the analysis was carried out in the time domain using a $2R(C + kUC(t))$ electric circuit powered by a direct current source I. Analytical equations are presented and comparisons between experimental and theoretical curves were made on a quantitative basis.

1. Introduction

Over the past years, extensive research has been concentrated on the investigation of electrochemical supercapacitors as energy storage devices due to their high relevance as exemplified in recent papers on the subject [1–14]. Their importance is even more conspicuous by the exceptional number of references cited on each of these publications. The development of new and better electrode materials and electrolytes has been the main focus of these studies. Measurement techniques have also been investigated to produce more reliable and comparative electrochemical and electrical data [15,16]. Modeling and simulation studies have also gaining growing attention [17–25].

Recently, time domain analytical expressions have been reported for the electrochemical supercapacitor with potential dependent capacitance derived considering short periods of charging and discharging processes as in cyclic voltammetry which is carried out in a few minutes [26]. Comparisons between such theoretical development and experimental cyclic voltammetry data have shown a very good agreement for carbon-based supercapacitors with organic electrolyte using a simple electrical circuit. Cyclic voltammetry and charge-discharge galvanostatic of supercapacitors are complementary to each other – quantities collected in one are not possible to be acquired by other such as capacitance and equivalent series resistance (ESR), respectively – and a similar study for the latter (charge-discharge galvanostatic) in the time domain is also of high relevance for modeling and simulations of these energy storage devices. Despite the recent effort in [26], similar studies in the time domain are inexistent in the literature for charge-discharge galvanostatic curves of supercapacitors.

Here the analytical equations governing a straightforward theoretical equivalent circuit of a symmetric electrochemical supercapacitor for charge-discharge galvanostatic curves, also including the capacitance dependent on the electrical potential, are presented. This is of special relevance since the degree of difficulty for obtaining equations for simulating the galvanostatic curves of supercapacitors is considerably impacted for electrical circuits in the time domain and by considering

* Corresponding author.
E-mail addresses: aprfff@usp.br (A.P.R. Fernandez), eaperigo@ieee.org (E.A. Périgo), rfaria@ipen.br (R.N. Faria).
[1] ABB US Research Center, Raleigh, NC 27606, USA.

https://doi.org/10.1016/j.est.2022.104471
Received 31 January 2022; Received in revised form 5 March 2022; Accepted 18 March 2022
Available online 28 March 2022

List of symbols

C is the fixed capacitance; unit: farad (F); is the capacitance obtained through the area of the voltammogram; unit: farad (F);
$EPR_{(AutDec)}$ is the equivalent parallel resistance obtained by the self-discharge method; unit: ohm (Ω);
I is the intensity of the electric current supplied by the direct current source I (in this case the galvanostat source), unit: ampere (A);
k is the incidence of capacitance dependent on the electrical potential, units: farads per volt (F V^{-1})
R_1 (ESR) represents equivalent series resistance, unit: ohm (Ω); is the series resistance obtained through the technique of abrupt variation of the electric potential; unit: ohm (Ω);
R_2 (EPR) represents equivalent series resistance, unit: ohm (Ω);
R_{Volt} is the internal resistance of the voltmeter used to evaluate the variation of the electric potential existing between the terminals of electrochemical supercapacitor during the self-discharge period; unit: ohm (Ω);
t is the elapsed time of the charging and discharging process of a supercapacitor; unit: second (s);
$t_{(iPC)}$ is the time at which the charge process initiates; unit: second (s);
$t_{(iPD)}$ is the time at which the discharge process initiates; unit: second (s);
$U(t)$ is the electric potential existing between the terminals of an electrochemical supercapacitor evaluated by means of the galvanostatic cycle technique at each moment of its charging or discharging process, unit: volt (V);
$U(t_{(fPAD)})$ is the electrical potential existing between the supercapacitor terminals at the end of the self-discharge process; unit: volt (V);
$U(t_{(iPAD)})$ is the electrical potential existing between the supercapacitor terminals at the beginning of the self-discharge process; unit: volt (V);
$U(t_{(iPC)})$ is the electric potential existing between the terminals of the electrochemical supercapacitor evaluated by means of the galvanostatic cycle technique at the beginning of its charge process, unit: volt (V);
$U(t_{(iPD)})$ is the electrical potential between the terminals of the electrochemical supercapacitor evaluated by means of the galvanostatic cycle technique at the beginning of its discharge process, unit: volt (V);
$U_C(t)$ is the electric potential existing between the terminals of the fixed capacitance capacitor C contained in the electrical circuit $2R(C + kU_C(t))$, unit: volt (V);
$U_C(t_{(iPC)})$ is the electric potential existing between the terminals of the fixed capacitance capacitor C contained in the electrical circuit $2R(C + kU_C(t))$ during its charge process carried out by a source of direct current I, unit: volt (V); and
$U_C(t_{(iPD)})$ is the electric potential existing between the terminals of the fixed capacitance capacitor C contained in the electrical circuit $2R(C + kU_C(t))$ during its discharge process; unit: volt (V)

the capacitance dependent on the potential. Experimental data have also been introduced in the general expressions to be compared with charge-discharge experimental galvanostatic curves of a carbon-based supercapacitor with organic electrolyte. As in the previous study on cyclic voltammetry [26], the analysis has been carried out in the time domain using a $2R(C + kU_C(t))$ electric circuit employing a current source for determining the equivalent series and parallel resistances, the fixed capacitance, and the electrical potential dependent capacitance index.

1.1. The equivalent circuits and time domain equations

Fig. 1 shows the $2R(C + kU_C(t))$ electric circuit powered by a source of direct current I. The $kU_C(t)$ electric component represents a capacitor with variable capacitance dependent on the electric potential on the capacitor with fixed capacitance C. Therefore, $kU_C(t)$ constitutes the capacitance which is dependent to the potential.

It can be verified for the process of charge of the fixed capacitance capacitor C present on the $2R(C + kU_C(t))$ circuit that:

$$U_C(t) = R_2 i_1(t), \tag{1}$$

just as:

$$i_1(t) = I - i_2(t) - i_3(t) \tag{2}$$

as well as:

$$i_2(t) = C\frac{d}{dt}U_C(t), \tag{3}$$

$$i_3(t) = kU_C(t)\frac{d}{dt}U_C(t). \tag{4}$$

Thus, it can be verified that:

$$U_C(t) = R_2\left(I - C\frac{d}{dt}U_C(t) - kU_C(t)\frac{d}{dt}U_C(t)\right), \tag{5}$$

$$\int \frac{C + kU_C(t)}{R_2 I - U_C(t)} dU_C(t) = \frac{1}{R_2}\int dt. \tag{6}$$

Integrating Eq. (6) results in:

$$(C + kR_2 I)ln(R_2 I - U_C(t)) - k(R_2 I - U_C(t)) + \frac{1}{R_2}t = c_1. \tag{7}$$

To obtaining the expression of the constant c_1 it is considered that for $t = t_{(iPC)}$ we have $U_C(t) = U_C(t_{(iPC)})$, which results in:

$$c_1 = (C + kR_2 I)ln\left(R_2 I - U_C\left(t_{(iPC)}\right)\right) - k\left(R_2 I - U_C\left(t_{(iPC)}\right)\right) + \frac{1}{R_2}t_{(iPC)}. \tag{8}$$

And with the appropriated substitutions:

$$t = t_{(iPC)} - R_2\left[(C + kR_2 I)ln\left(\frac{R_2 I - U_C(t)}{R_2 I - U_C\left(t_{(iPC)}\right)}\right) + k\left(U_C(t) - U_C\left(t_{(iPC)}\right)\right)\right]. \tag{9}$$

Eq. (9) makes it possible to calculate the theoretical values of t as a function of the experimental values of the electrical potential $U_C(t)$ for the charging process of an fixed capacitance capacitor C contained in circuit $2R(C + kU_C(t))$ powered by a direct current source I. It is not possible to evaluate the potential $U_C(t)$ of an electrochemical supercapacitor, whether symmetrical or not; nevertheless, it is perfectly possible to evaluate the intensity of the electric current present in the branch that connects it to the direct current source I, just as it is possible to evaluate the electric potential $U(t)$ existing between the terminals of the supercapacitor. Therefore, considering that:

$$U(t) = R_1 I + R_2 i_1(t), \tag{10}$$

and

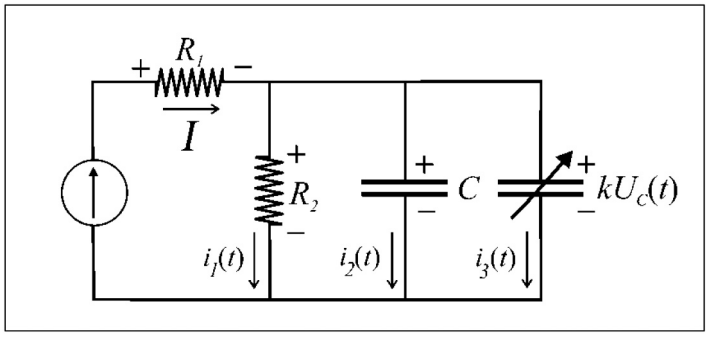

Fig. 1. $2R(C + kU_C(t))$ electrical circuit powered by a direct current source on the charging process of the capacitor with fixed capacitance C.

$$i_1(t) = \frac{1}{R_2}U_C(t), \tag{11}$$

one obtains:

$$U_C(t) = U(t) - R_1 I. \tag{12}$$

Substituting Eq. (12) on Eq. (9), as well as considering that:

$$U_C\left(t_{(iPC)}\right) = U\left(t_{(iPC)}\right) - R_1 I, \tag{13}$$

it can be verified that:

$$t = t_{(iPC)} - R_2\left[(C + kR_2 I)ln\left(\frac{(R_2 + R_1)I - U(t)}{(R_2 + R_1)I - U\left(t_{(iPC)}\right)}\right) + k\left(U(t) - U\left(t_{(iPC)}\right)\right)\right]. \tag{14}$$

Eq. (14) makes it possible to calculate the theoretical values of t as a function of the experimental values of $U(t)$ obtained by analyzing the charging process of a symmetric electrochemical supercapacitor evaluated by means of the galvanostatic cycle technique.

It follows that the initial values of R_1 (*ESR*), R_2 (*EPR*), C and k can be obtained by other techniques used in the analysis of electrochemical supercapacitors, as examples are the capacitance obtained by means of the area of the voltammogram by the cyclic voltammetry technique, and the *ESR* value by the abrupt change of electric potential that occurs in the galvanostatic cycle technique. Such initial values can also be "selected at random" and, later, adjusted until the best possible result is obtained, which, as stated, is the smallest value of the sum of the modules of the differences between the theoretical and experimental values of t. After obtaining the adequate theoretical values of t, it is enough to formulate a table of the theoretical values as a function of the experimental values of $U(t)$ and, with it, performing the inversion of the axes to generate the simulation graph of the dependent variable $U(t)$ as a function of the independent variable t.

Subsequently, taking Fig. 2 for instance, which shows the direction of displacement of the electrical charges contained in the respective electrical currents I, $i_1(t)$, $i_2(t)$ and $i_3(t)$, it would be obtained the equation

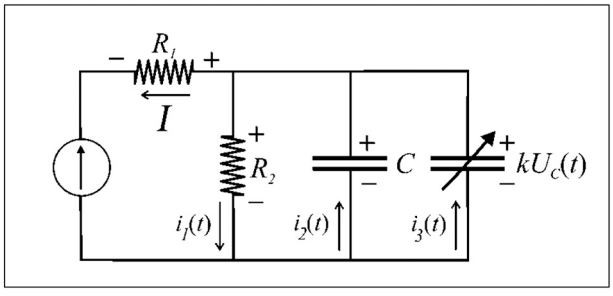

Fig. 2. Current displacement directions on $2R(C + kU_C(t))$ electrical circuit on the charging process of the capacitor with fixed capacitance C.

that makes it possible to calculate the theoretical values of t as a function of the experimental values of $U(t)$ for the discharge process of a supercapacitor evaluated by means of the galvanostatic cycle technique.

For the discharge process of the capacitor C on the electrical circuit $2R(C + kUC(t))$, according to Fig. 2, follows that:

$$U(t) = -R_1 I + R_2 i_1(t). \tag{15}$$

since that:

$$U_C(t) = R_2 i_1(t). \tag{16}$$

Similarly, for the discharge process it can be verified that:

$$I + i_1(t) = i_2(t) + i_3(t), \Rightarrow \tag{17}$$

$$i_1(t) = i_2(t) + i_3(t) - I. \tag{18}$$

for the discharge process of the capacitor with fixed capacitance C it follows that:

$$i_2(t) = -C\frac{d}{dt}U_C(t), \tag{19}$$

$$i_3(t) = -kU_C(t)\frac{d}{dt}U_C(t). \tag{20}$$

Thus, it is verified that:

$$\int \frac{C + kU_C(t)}{U_C(t) + R_2 I} dU_C(t) = -\frac{1}{R_2}\int dt, \tag{21}$$

Solving the integrals on this equation it is obtained:

$$(C - kR_2 I)ln(R_2 I + U_C(t)) + k(R_2 I + U_C(t)) + \frac{1}{R_2}t = c_2. \tag{22}$$

For obtaining the expression of the constant c_2 it is considered that when $t = t_{(iPD)}$ then $U_C(t) = U_C(t_{(iPD)})$, resulting that:

$$c_2 = (C - kR_2 I)ln\left(R_2 I + U_C\left(t_{(iPD)}\right)\right) + k\left(R_2 I + U_C\left(t_{(iPD)}\right)\right) + \frac{1}{R_2}t_{(iPD)}. \tag{23}$$

Thus, replacing the term to the right of Eq. (23) in Eq. (22) and considering for the discharge process that:

$$U_C(t) = U(t) + R_1 I, \tag{24}$$

so that:

$$U_C\left(t_{(iPD)}\right) = U\left(t_{(iPD)}\right) + R_1 I, \tag{25}$$

it is verified that:

$$t = t_{(iPD)} - R_2\left[(C - kR_2 I)ln\left(\frac{U(t) + (R_2 + R_1)I}{U\left(t_{(iPD)}\right) + (R_2 + R_1)I}\right) + k\left(U(t) - U\left(t_{(iPD)}\right)\right)\right]. \tag{26}$$

Eq. (26) makes it possible to calculate the theoretical values of t as a function of the experimental values of $U(t)$ obtained in the discharge process of an electrochemical supercapacitor evaluated by means of the galvanostatic cycle technique. As previously, having available the appropriate theoretical values of t, it is enough to create the table of the theoretical values of t as a function of the experimental values of $U(t)$ and with it performing the inversion of the axes and generating the graph of simulation of the dependent variable $U(t)$ as a function of the independent variable t.

The value of the equivalent series resistance of a symmetrical electrochemical supercapacitor, represented by R_1 in the electrical circuits shown in Figs. 1 and 2, can be obtained considering that the intensity of the electric current I and the electric potential $U_C(t)$ on the capacitor C in the electrical circuit $2R(C + kU_C(t))$ are maintained during the shortest time interval in which the change between the processes from charge to discharge of this electrical component occurs, as well as considering that in such a short time interval there is an abrupt variation of the electric potential $U(t)$ on the terminals of the electric circuit $2R(C + kU_C(t))$, as occurs with an electrochemical supercapacitor evaluated using the galvanostatic cycle technique.

Thus, considering that:

$$U_C\left(t_{(fPC)}\right) = U\left(t_{(fPC)}\right) - R_1 I, \tag{27}$$

also that:

$$U_C\left(t_{(iPD)}\right) = U\left(t_{(iPD)}\right) + R_1 I, \tag{28}$$

it is verified that:

$$U\left(t_{(fPC)}\right) - R_1 I = U\left(t_{(iPD)}\right) + R_1 I, \tag{29}$$

$$ESR = \frac{U\left(t_{(fPC)}\right) - U\left(t_{(iPD)}\right)}{2I}. \tag{30}$$

Eq. (30) allows calculating the value of R_1 (ESR) of a symmetrical electrochemical supercapacitor.

2. Experimental

The experimental part of this study was carried out using a commercial symmetrical electrochemical supercapacitor based on carbon and organic electrolyte as a reference. The supercapacitor (nominal ratings: 1F – 5.5 V) was composed by two series coin cells and only one coin cell was used in the galvanostatic charge-discharge measurements. Thus, the specification of one cell was 2 F and a maximum operating potential of 2.75 V. Only this single coin cell has been measured. Due the high conductivity, common electrolytes in these cells are tetraethylammonium tetrafluoroborate salt (NEt_4BF_4) in acetonitrile (ACN) or propylene carbonate (PC) [27].

The galvanostatic cycles were performed using the Arbin BT4 with MITSPRO software equipment operating as a galvanostat with a charge and discharge current of 5 mA, 10 mA and 14 mA which was maintained until the electrical potential on the terminals of the supercapacitor cell reached a value of 2.6 V. The inversion of the direction of displacement of the electric charges present in the electric current I occurs automatically and instantaneously, with a discharge intensity of 10 mA, and this condition remains until the moment in which the electric potential between the coin cell terminals becomes 0 V, starting a new charge and discharge cycle. The value of the equivalent series resistance was calculated using Eq. (30). The theoretical and experimental values of t used to plot the curves and the sum of the modules of the differences between such values was used as overlapping estimation.

The ESR (R_1), EPR (R_2), C and k values were obtained by consecutive adjustments, with three of these fundamental electrical parameters being kept fixed, while one is modified (changed) until the best overlapping result is obtained. The value of the fundamental electrical parameter to be determined is initially chosen at random and inserted into the equations that make it possible to obtain the theoretical values of t for the charging and discharging processes of the fixed capacitance capacitor C.

Subsequently, the evaluation of the result of such choice is carried out by means of the sum of the modules of the differences between the theoretical and experimental values of t. Then, another value very close to the one previously chosen is inserted and it is verified whether the new value has increased or reduced the value of the sum of the modules of the differences between the theoretical and experimental values of t. This process is carried out until the lowest possible value of the sum of the modules of the differences between the theoretical and experimental values of t is obtained.

Next, another fundamental parameter is taken as a study variable, fixing the value of the others. The process of determining the value of the fundamental parameter under study is carried out, once again, by evaluating the convergence to the lowest possible value of the sum of the modules of the differences between the theoretical and experimental values of t. Sometimes it is necessary to perform two or more adjustment cycles.

In this investigation, cyclic voltammetry (used in a previous simulation study [26]) has also been carried out as complement to galvanostatic cycling. Self-discharge resistance was obtained using the following equation:

$$EPR_{(AutDesc)} = \frac{R_{Volt} + ESR}{(R_{Volt} + ESR)\frac{C}{t} ln\left(\frac{U\left(t_{(iPAD)}\right)}{U\left(t_{(fPAD)}\right)}\right) - 1}. \tag{31}$$

3. Results and discussion

Fig. 3 shows the experimental curves of $U(t)$ as a function of t (galvastatic curves - black line) generated by the charging and discharging processes of the commercial electrochemical supercapacitor of nominal capacitance of 2 F at an electric current of 10 mA and the electric current indication curve (blue continuous line).

Using Eq. (30) and taking as a reference the values of the abrupt variation of the electric potential from 2.60 V ($U(t_{(fPC)})$) to 2.43 V ($U(t_{(iPD)})$), which occurred when switching from the charging process to the discharging process of the electrochemical supercapacitor with nominal capacitance of 2 F, as shown in Fig. 4 (enlargement of the peak region of the curve presented through Fig. 3), the ESR value ($R1$) of approximately 20 Ω was obtained.

Subsequently, inserting in Eqs. (14) and (26) the parameters R_1 =

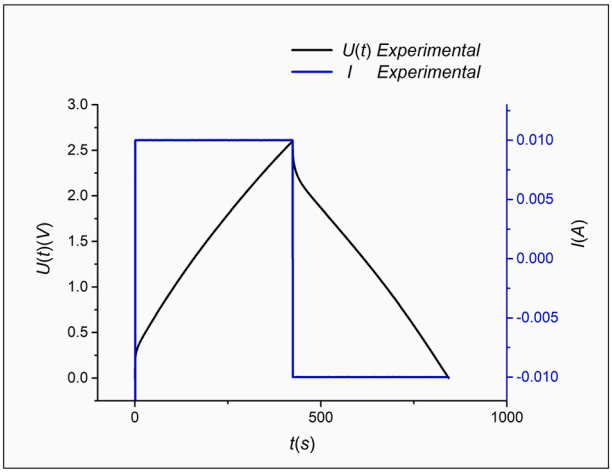

Fig. 3. Galvanostatic curve of a commercial symmetric electrochemical supercapacitor with nominal capacitance of 2 F charged to a maximum potential of 2.6 V. Charging-discharging performed with a current I of constant intensity in time of 10 mA.

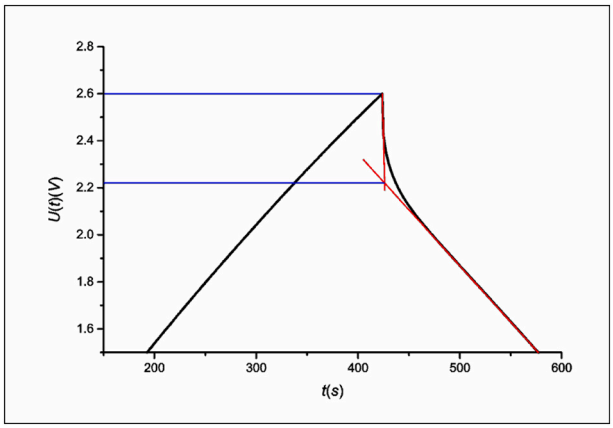

Fig. 4. Details of the galvanostatic curve generated by the analysis of a commercial 2 F supercapacitor when the direction of displacement of the electric charges in the electric current I of 10 mA is changed and the consequent abrupt variation of the electric potential.

19.50 Ω, $R_2 = 243$ Ω, $C = 2$ F, $k = 0$, $I = 10$ mA, $t_{(iPC)} = 1.07$ s, $U(t_{(iPC)}) = 0.23$ V, $t_{(iPD)} = 424.85$ s and $U(t_{(iPD)}) = 2.23$ V and the experimental values of $U(t)$, the theoretical values of t were readily obtained, and with these theoretical galvanostatic curves were generated for the charge and the discharge processes for the supercapacitor with nominal capacitance of 2 F, as shown in Fig. 5. The value of 243 Ω of parameter R_2 was then determined, as it is the smallest value that can be inserted into Eqs. (14) and (26) in accordance with the other parameters chosen without distortions in the galvanostatic load and discharge generated by them. The parameter C was taken as being equal to 2 F, as this is the value of the nominal capacitance of the commercial electrochemical supercapacitor evaluated by the galvanostatic cycle technique and, finally, the parameter k was taken as being null, as there was interest in verifying how the capacitance index dependent on the electric potential acts on the galvanostatic curves, in addition to the fact that this parameter has not been evaluated by another technique.

In Fig. 5 the electric potential seems to "travel in time" because in the previous equations there is no way to isolate $U(t)$, so the theoretical values of t are obtained based on the experimental values of $U(t)$, and the axes are inverted, obtaining the "false" graph of $U(t)$ as a function of t, but in fact what is obtained is a graph of t as a function of $U(t)$ inverted. In this way it appears that the electric potential goes to the future and then back to the past, but what actually happens is that the electric potential $U(t)$ has undergone an abrupt change in intensity.

Taking as a reference the theoretical and experimental values of t used to plot the curves presented in Fig. 5, it was found that the sum of the modules of the differences between such values resulted in approximately 203,286 s.

Then, by free choice, the parameters $R_1 = 19.50$ Ω, $R_2 = 60$ kΩ, $C = 2$ F, $k = 0$, $I = 10$ mA, $t_{(iPC)} = 1.07$ s, $U(t_{(iPC)}) = 0.23$ V, $t_{(iPD)} = 424.85$ s and $U(t_{(iPD)}) = 2.23$ V were inserted in Eqs. (14) and (26) and the result is shown in Fig. 6. In accordance with the theoretical values of t contained in Fig. 6, it was found that the sum between the modules of the differences of such values and the respective experimental values was approximately 26,590 s, indicating a reduction of 176,696 s compared to the value calculated previously.

Then, inserting the parameters $R_1 = 19.50$ Ω, $R_2 = 60$ kΩ, $C = 1.80$ F, $k = 0$, $I = 10$ mA, $t_{(iPC)} = 1.07$ s, $U(t_{(iPC)}) = 0.23$ V, $t_{(iPC)} = 424.85$ s and $U(t_{(iPD)}) = 2.23$ V in the equations that make it possible to calculate the theoretical values of t as a function of the experimental values of $U(t)$ obtained by the processes of charge and discharge of a symmetrical supercapacitor evaluated by means of the cyclic voltammetry technique, theoretical galvanostatic curves were generated for the new configuration of electrical parameters, as shown in Fig. 7. In this case the sum of the modulus of the differences between the theoretical and experimental values of t was approximately 21,020 s.

As can be seen, the values $R_1 = 19.50$ Ω, $R_2 = 60$ kΩ, $C = 1.80$ F, $k = 0$, $I = 10$ mA, $t_{(iPC)} = 1.07$ s, $U(t_{(iPC)}) = 0.23$ V, $t_{(iPC)} = 424.85$ s and $U(t_{(iPD)}) = 2.23$ V ended up generating more theoretical curves closer to the experimental ones. After some successive approximations it was found that the values $R_1 = 19.50$ Ω, $R_2 = 80$ kΩ, $C = 1.45$ F, $k = 0.25$ F V^{-1}, $I = 10$ mA, $t_{(iPC)} = 1.07$ s, $U(t_{(iPC)}) = 0.23$ V, $t_{(iPD)} = 424.85$ s and $U(t_{(iPD)}) = 2.23$ V, resulted in the smallest value of the sum of the modules of the differences between the theoretical and experimental values of t, as can be seen in Fig. 8.

In accordance with the parameters $R_1 = 19.50$ Ω, $R_2 = 80$ kΩ, $C = 1.33$ F, $k = 0.39$ F V^{-1}, $I = 10$ mA, $t_{(iPC)} = 1.07$ s, $U(t_{(iPC)}) = 0.23$ V, $t_{(iPD)} = 424.85$ s and $U(t_{(iPD)}) = 2.23$ V, the smallest possible value of the sum of the modules of the differences between the theoretical and

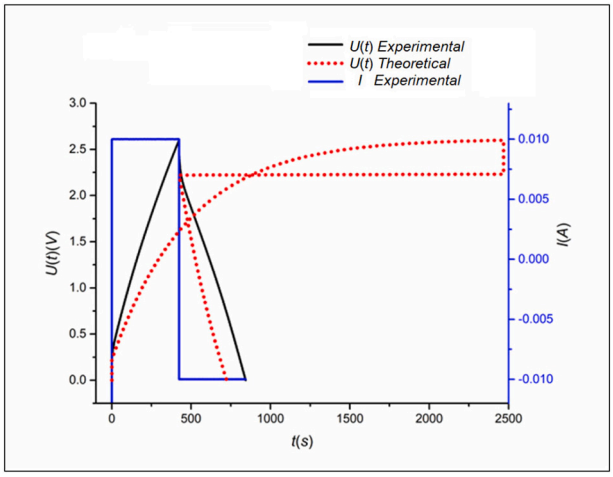

Fig. 5. Comparison between experimental (black continuous line) and theoretical (red dotted line) galvanostatic curves considering that the theoretical curves were plotted through Eqs. (14) and (26), in which the following parameters were inserted $R_1 = 19.50$ Ω, $R_2 = 243$ Ω, $C = 2$ F, $k = 0$, $I = 10$ mA, $t_{(iPC)} = 1.07$ s, $U(t_{(iPC)}) = 0.23$ V, $t_{(iPD)} = 424.85$ s and $U(t_{(iPD)}) = 2.23$ V. (For interpretation of the references to color in this figure legend, the reader is referred to the web version of this article.)

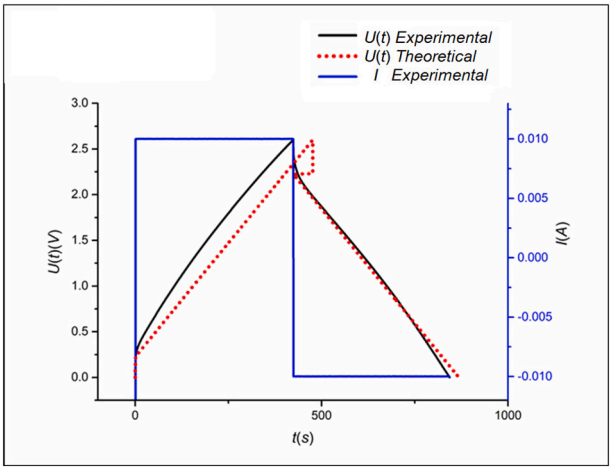

Fig. 6. Comparison between experimental (black continuous line) and theoretical (red dotted line) galvanostatic curves considering that the theoretical curves were plotted using Eqs. (14) and (26), in which the following parameters were inserted $R_1 = 19.50$ Ω, $R_2 = 60$ kΩ, $C = 2$ F, $k = 0$, $I = 10$ mA, $t_{(iPC)} = 1.07$ s, $U(t_{(iPC)}) = 0.23$ V, $t_{(iPD)} = 424.85$ s and $U(t_{(iPD)}) = 2.23$ V. (For interpretation of the references to color in this figure legend, the reader is referred to the web version of this article.)

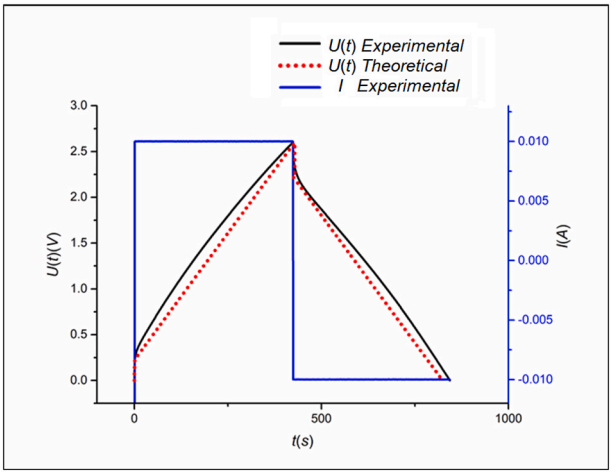

Fig. 7. Comparison between experimental (black continuous line) and theoretical (red dotted line) galvanostatic curves considering $R_1 = 19.50\ \Omega$, $R_2 = 60$ kΩ, $C = 1.80$ F, $k = 0$, $I = 10$ mA, $t_{(iPC)} = 1.07$ s, $U(t_{(iPC)}) = 0.23$ V, $t_{(iPC)} = 424.85$ s and $U(t_{(iPD)}) = 2.23$ V using Eqs. (14) and (26). (For interpretation of the references to color in this figure legend, the reader is referred to the web version of this article.)

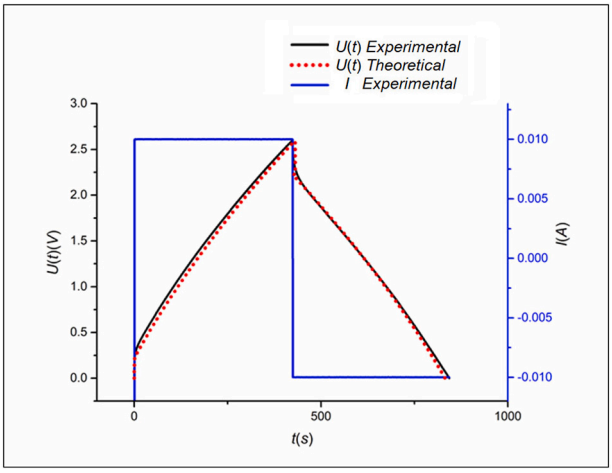

Fig. 9. Comparison between experimental (black continuous line) and theoretical (red dotted line) galvanostatic curves considering $R_1 = 19.50\ \Omega$, $R_2 = 80$ kΩ, $C = 1.33$ F, $k = 0.39$ F V^{-1}, $I = 10$ mA, $t_{(iPC)} = 1.07$ s, $U(t_{(iPC)}) = 0.23$ V, $t_{(iPD)} = 424.85$ s and $U(t_{(iPD)}) = 2.23$ V. (For interpretation of the references to color in this figure legend, the reader is referred to the web version of this article.)

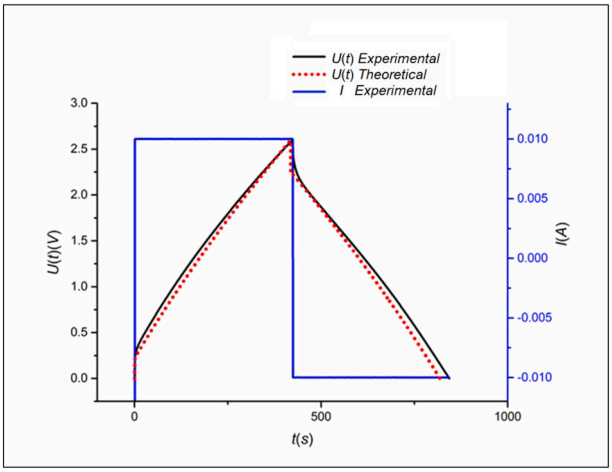

Fig. 8. Comparison between experimental (black continuous line) and theoretical (red dotted line) galvanostatic curves considering $R_1 = 19.50\ \Omega$, $R_2 = 80$ kΩ, $C = 1.45$ F, $k = 0.25$ F V^{-1}, $I = 10$ mA, $t_{(iPC)} = 1.07$ s, $U(t_{(iPC)}) = 0.23$ V, $t_{(iPD)} = 424.85$ s and $U(t_{(iPD)}) = 2.23$ V, using Eqs. (14) and (26). (For interpretation of the references to color in this figure legend, the reader is referred to the web version of this article.)

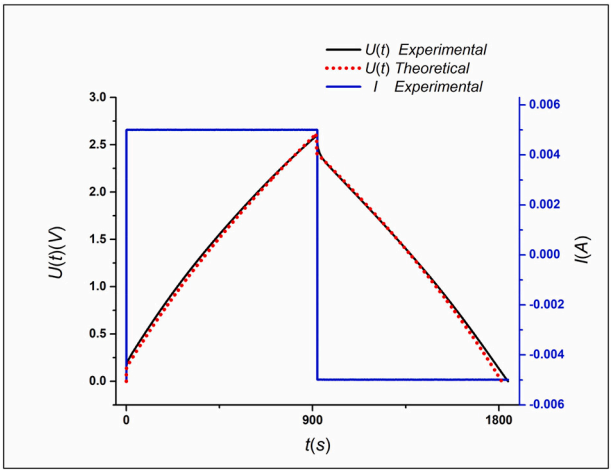

Fig. 10. Comparison between experimental (black continuous line) and theoretical (red dotted line) galvanostatic curves considering $R_1 = 19\ \Omega$, $R_2 = 100$ kΩ, $C = 1.35$ F, $k = 0.39$ F V^{-1}, $I = 5$ mA, $t_{(iPC)} = 1.07$ s, $U(t_{(iPC)}) = 0.14$ V, $t_{(iPD)} = 937.29$ s and $U(t_{(iPD)}) = 2.40$ V. (For interpretation of the references to color in this figure legend, the reader is referred to the web version of this article.)

experimental values of t of about 5905 s was obtained, for a total of 840 analysis points, being the comparative result between the theoretical galvanostatic curve generated by such values and the experimental curve presented through Fig. 9.

Fig. 10 shows a comparison between the experimental galvanostatic curve of the supercapacitor with nominal capacitance of 2 F using a current of only 5 mA and the theoretical curves obtained using Eqs. (14) and (26). The theoretical curves were generated by the values of R_1 (*ESR*), R_2 (*EPR*), C and k that produced the smallest possible value of the sum of the modules of the differences between the experimental and theoretical values of t. It was found that the smallest possible value of the sum of the modules of the differences between the experimental and theoretical values was approximately 18,513 s for a total of 1844 analyzed points. Fig. 11 shows a detailed view of the initial potential drop of the curve shown in Fig. 10 using Eq. (30). In this case, with a current of 5 mA, the *ESR* (R_1) is 19 Ω.

Fig. 12 shows a similar comparison of the supercapacitor with nominal capacitance of 2 F using a current of 14 mA. In this case, it was found that the smallest possible value of the sum of the modules of the differences between the experimental and theoretical values was approximately 1618 s for a total of 547 analyzed points. Fig. 13 shows the detail of the inflection point (abrupt drop in electrical potential) presented in Fig. 12 using a charge/discharge current of 14 mA. The ESR (R_1) in accordance with Eq. (30) was approximately 17.85 Ω.

Fig. 14 shows that the value of the fixed capacitance obtained by the area of the voltammogram generated at a scan rate of 5 mV s^{-1} of supercapacitor with nominal capacitance of 2 F is about 1.74 F. Similarly, Fig. 15 shows that the value of the fixed capacitance obtained at a scan rate of 10 mV s^{-1} is about 1.56 F. Increasing the scan rate to 50 mV s^{-1} further decreases the fixed capacitance to 0.5 F, as shown in Fig. 16.

For a total of 200 h of self-discharge and considering the highest capacitance value obtained through the voltammogram area (1.74 F), as well as considering that the *ESR* value is approximately 20 Ω, and the

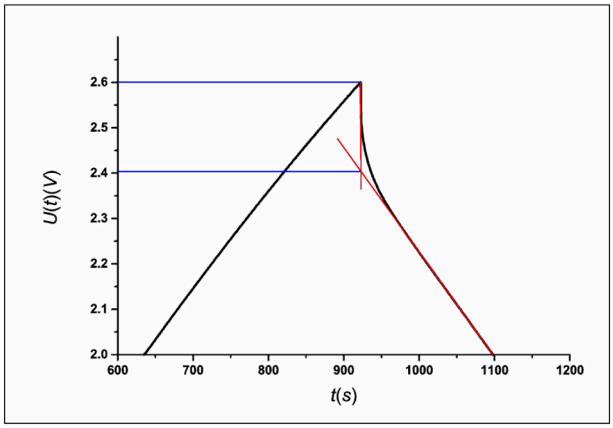

Fig. 11. Detailed view of the initial potential drop on reversing a current of 5 mA and employing Eq. (30).

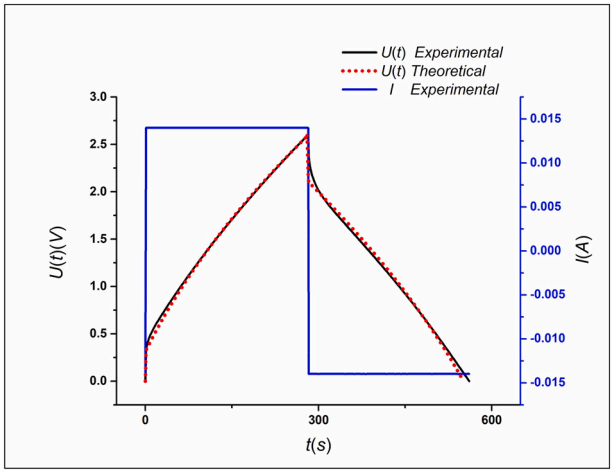

Fig. 12. Comparison between experimental (black continuous line) and theoretical (red dotted line) galvanostatic curves considering $R_1 = 17.85\ \Omega$, $R_2 = 10$ kΩ, $C = 1.12$ F, $k = 0.51$ F V^{-1}, $I = 14$ mA, $t_{(iPC)} = 1.07$ s, $U(t_{(iPC)}) = 0.32$ V, $t_{(iPD)} = 283.02$ s and $U(t_{(iPD)}) = 2.10$ V. (For interpretation of the references to color in this figure legend, the reader is referred to the web version of this article.)

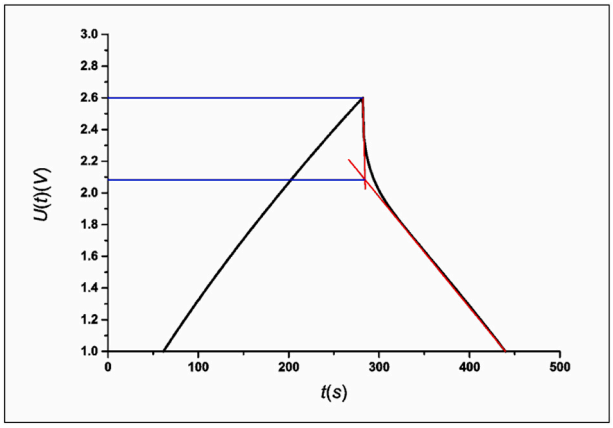

Fig. 13. Detailed view of the initial potential drop on reversing a current of 14 mA and employing Eq. (30).

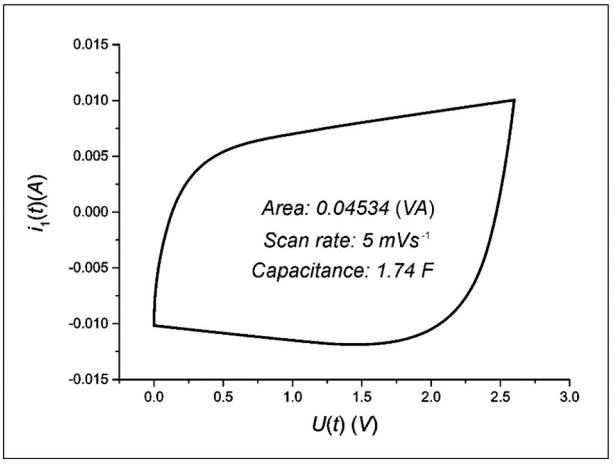

Fig. 14. Voltamogram with area of 0.04534 (VA) obtained at a scan rate of 5 mV s^{-1} on evaluating the symmetric electrochemical supercapacitor with nominal capacitance of 2 F.

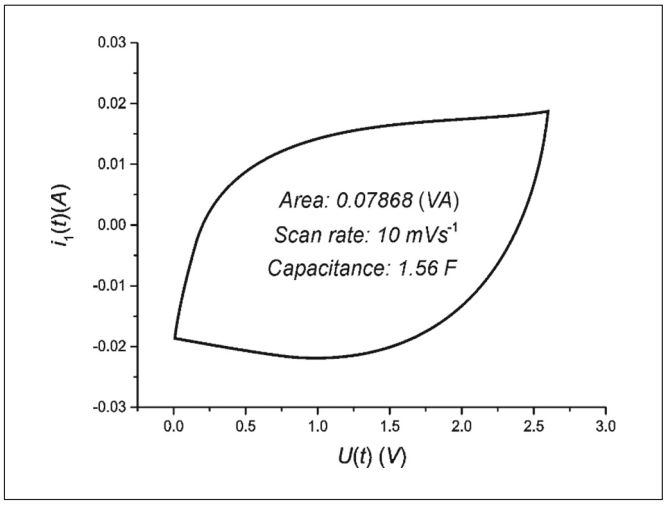

Fig. 15. Voltamogram with area of 0.07868 (VA) obtained at a scan rate of 10 mV s^{-1} on evaluating the symmetric electrochemical supercapacitor with nominal capacitance of 2 F.

value of 10 MΩ of the internal resistance of the voltmeter used to evaluate the variation of the electric potential existing between the terminals of the electrochemical supercapacitor, it was verified that the value of the *EPR* (R_2) of the symmetric electrochemical supercapacitor with nominal capacitance of 2 F was of approximately 403 kΩ (which is an adequate value for a total of 200 h of self-discharge).

The aim of this paper was to demonstrate that it is possible to simulate, even if roughly, the behavior of an electrochemical supercapacitor through a straightforward electrical circuit that makes it possible to include the capacitance dependent on the electrical potential in equations that allow yielding the experimental curves. This electrical circuit is too simplistic (and this is its main advantage) since, for instance, it does not consider the effects of temperature (or even, the interaction between electrolyte and electrode at the interface, or the variation of the ionic concentration from the electrolyte bulk to the electrode/electrolyte interface region).

However, the absence of terms that would allow evaluating the effects of temperature, or ionic concentration at the electrode/electrolyte interface, in addition to other input variables that were not computed, is verified by the resulting value of the sum module of the differences between the experimental and theoretical values of t, which will never

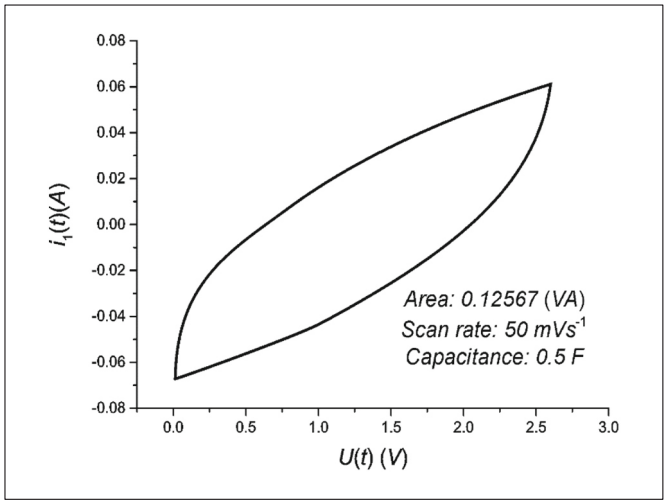

Fig. 16. Voltamogram with area of 0.12567 (VA) obtained at a scan rate of 50 mV s^{-1} when evaluating the symmetric electrochemical supercapacitor with a nominal capacitance of 2 F.

be null precisely because such input variables are not computed. It mean then that the higher the sum, less incomplete is the model in terms of variables considered. It is worth mentioning that as other terms are added to the 2R(C + kUC(t)) circuit, the equations that allow simulating the response variables become increasingly complex. Further developments are planned to include additional influences of not-considered variables by now.

In order to compare the *ESR*, *EPR* and *C* values obtained through the smallest possible value of the sum of the modulus of differences between the experimental and theoretical values of *t* with other trends, which aims to verify disparities, the ESR values are obtained through the abrupt drop of the electric potential. This is verified in the technique of the galvanostatic cycle for different values of electric current of charge and discharge. The value of the *EPR* is obtained through the technique of self-discharge and the value of the capacitance is obtained through of the voltammogram area.

Time-domain analysis techniques, such as the galvanostatic cycle technique, need to be complemented by frequency-domain techniques, such as the electrochemical impedance electrochemical spectroscopy (EIS) technique. The latter can evaluate the effects of the electrical input inductance *L* which, although rare, can cause changes in the response behavior of electrochemical supercapacitors when they are used with alternating electrical sources. EIS can easily detect the presence of the input inductance through the Nyquist and Bode diagrams of the complex impedance module. It can detect the negative of the lag angle existing between the intensity of the electric current and the electric potential present at the terminals of the supercapacitor. EIS should also be used since it allows evaluating the complex capacitance [27].

4. Conclusions

The analytical equations that successfully simulate the charge and discharge of galvanostatic curves of a symmetrical electrochemical supercapacitor based on carbon and organic electrolyte have been deduced. The equations obtained via the analysis in the time domain of the electrical circuit $2R(C + kUC(t))$ powered by a direct current source *I* were able to simulate with good similarity the theoretical curves of a nominal capacitance of 2 F commercial supercapacitor evaluated by the galvanostatic cycle technique. This has been based on the fact that the sum of the modules of the differences between the theoretical and experimental values of *t*. The best result of approximation between theoretical and experimental curves was approximately 5905 s, with such comparative parameter being about to 203,286 s before the adjusted values of R_1, R_2, *C* and *k*. The results were obtained by inserting optimum values ($R_1 = 20\ \Omega$, $R_2 = 80\ k\Omega$, $C = 1.33$ F and $k = 0.39\ F\ V^{-1}$, $I = 10$ mA, $t_{(iPC)} = 1.07$ s, $U(t_{(iPC)}) = 0.23$ V, $t_{(iPD)} = 424.85$ s and $U(t_{(iPD)}) = 2.23$ V) in the equations deduced to simulate the experimental curves for the charge and discharge processes of a supercapacitor evaluated by means of the galvanostatic cycle technique. As a comparative basis *t* values were obtained through the analyses of a commercial 2 F supercapacitor powered by the current of a galvanostat (10 mA). Obtaining the electrical parameters *ESR*, *EPR*, *C* and *k* quantitatively by the smallest possible value of the sum of the modules of the differences between theoretical and experimental values of *t* can be considered an advantageous "technique" as it represents a reduction of costs and time. With it is possible to obtain at once such fundamental electrical parameters of supercapacitors, which requires the use of other analysis techniques such as cyclic voltammetry.

Declaration of competing interest

The authors declare that there is no conflict of interest.

Acknowledgments

The work of A. P. R. Fernandez was supported by SENAI-SP, São Paulo, Brazil.

References

[1] F.A. Latif, N.A.M. Zailani, Z.S.M.A. Shukaili, S.F.M. Zamri, N.A.M. Kasim, M.S. A. Rani, M.N.F. Norrrahim, Review of poly (methyl methacrylate) based polymer electrolytes in solid-state supercapacitors, Int. J. Electrochem. Sci. 17 (2022), 22013, https://doi.org/10.20964/2022.01.44.

[2] M. Yaseen, M.A.K. Khattak, M. Humayun, M. Usman, S.S. Shah, S.B.B.S. Hasnain, S. M. Ahmad, A. Khan, N. Shah, A.A. Tahir, H. Ullah, A review of supercapacitors: materials design, modification, and applications, Energies 14 (2021) 7779, https://doi.org/10.3390/en14227779.

[3] G.S.D. Reis, H.P.O. Oliveira, S.H. Larsson, M. Thyrel, E.C. Lima, A short review on the electrochemical performance of hierarchical and nitrogen-doped activated biocarbon-based electrodes for supercapacitors, Nanomaterials 11 (2021) 424, https://doi.org/10.3390/nano11020424.

[4] H. Lv, Q. Pan, Y. Song, X. Liu, T. Liu, H. Lv, Q. Pan, A review on nano-/microstructured materials constructed by electrochemical technologies for supercapacitors, Nano-Micro Lett. 12 (2020) 118, https://doi.org/10.1007/s40820-020-00451-z.

[5] S. Mukhopadhyay, R. Dhaouadi, M. Takrouri, R. Dogga, Supercapacitor characterization using universal adaptive stabilization and optimization, IEEE Open J. Ind. Electron. Soc. 1 (2020) 166–183, https://doi.org/10.1109/OJIES.2020.3008339.

[6] S. Zheng, Q. Li, H. Pang, Q. Xu, H. Xue, A highly alkaline-stable metal oxide@metal–organic framework composite for high-performance electrochemical energy storage, Natl. Sci. Rev. 7 (2020) 305–314, https://doi.org/10.1093/nsr/nwz137.

[7] P. Zhu, X. Li, H. Yao, H. Pang, Hollow cobalt-iron prussian blue analogue nanocubes for high-performance supercapacitors, J. Energy Storage 31 (2020), 101544, https://doi.org/10.1016/j.est.2020.101544.

[8] A. Deepak, C. Pheba, Types of supercapacitors and benefits of graphene and its derivatives as electrodes, Res. J. Chem. Environ. 24 (11) (2020) 158–167.

[9] Z. Liang, R. Zhao, T. Qiu, R. Zou, Q. Xu, Metal-organic framework-derived materials for electrochemical energy applications, EnergyChem 1 (1) (2019), 100001, https://doi.org/10.1016/j.enchem.2019.100001.

[10] M. Ciszewski, A. Koszorek, T. Radko, P. Szatkowski, D. Janas, Review of the selected carbon-based materials for symmetric supercapacitor application, J. Electron. Mater. 48 (2) (2019), https://doi.org/10.1007/s11664-018-6811-7.

[11] M. Aghazadeh, Cathodic electrochemical deposition of nanostructured metal oxides/hydroxides and their composites for supercapacitor applications: a review, Anal. Bioanal. Electrochem. 11 (2) (2019) 211–266.

[12] S.Y.S. Kou, Recent advances of flexible electrospun nanofibers-based electrodes for electrochemical supercapacitors: a minireview, Int. J. Electrochem. Sci. 14 (2019) 7811–7831, https://doi.org/10.20964/2019.08.28.

[13] Q. Qi Li, M. Horn, Y. Wang, J. MacLeod, N. Motta, J. Liu, A review of supercapacitors based on graphene and redox-active organic materials, Materials 12 (2019) 703, https://doi.org/10.3390/ma12050703.

[14] A. Berrueta, A. Ursúa, L.S. Martin, A. Eftekhari, P. Sanchis, Supercapacitors: electrical characteristics, modeling, applications, and future trends, special section on advanced energy storage technologies and their applications, IEEE Access 7 (2019) 50869–50896.

[15] R. Vicentini, L.M. Silva, E.P.C. Junior, T.A. Alves, Nunes, W.G.H. Zanin, How to measure and calculate equivalent series resistance of electric double-layer capacitors, Molecules 24 (2019) 1452, https://doi.org/10.3390/molecules24081452.

[16] S. Zhang, N. Pan, Supercapacitors performance evaluation, Adv. Energy Mater. 1401401 (2014) 1–19, https://doi.org/10.1002/aenm.201401401.
[17] M.A.B. Fathallah, A.B. Othman, M. Besbes, Modeling a photovoltaic energy storage system based on super capacitor, simulation and evaluation of experimental performance, Appl. Phys. A (2018) 120–124.
[18] L.E. Helseth, Modelling supercapacitors using a dynamic equivalent circuit with a distribution of relaxation times, J. Energy Storage 25 (2019), 100912.
[19] I.N. Jiya, N. Gurusinghe, R. Gouws, Electrical circuit modelling of double layer capacitors for power electronics and energy storage applications: a review, Electronics 7 (2018) 268, https://doi.org/10.3390/electronics7110268.
[20] Y. Parvini, J.B. Siegel, A.G. Stefanopoulou, A. Vahidi, Supercapacitor electrical and thermal modeling, identification, and validation for a wide range of temperature and power applications, IEEE Trans. Ind. Electron. 63 (3) (2016) 1574–1585.
[21] P.O. Logerais, M.A. Camara, A. Djellad, A. Omeiri, F. Delaleux, J.F. Durastanti, in: Modeling of a Supercapacitor With a Multibranch Circuit 40, 2015, pp. 13725–13736, 39.
[22] S.A. Kim, W. Choi, K. Lee, S. Choi, Advanced dynamic simulation of supercapacitors considering parameter variation and self-discharge, IEEE Trans. Power Electron. 26 (11) (2011) 3377–3385.
[23] D. Petreus, D. Moga, R. Galatus, A. Munteanu, Modeling and sizing of supercapacitors, Adv. Electr. Comput. Eng. 8 (2) (2008) 15–22.
[24] L. Zhang, Z. Wang, X. Hu, F. Sun, D.G. Dorrell, A review of supercapacitor modeling, estimation, and applications: a control/management perspective, J. Power Sources 274 (2015) 899–906.
[25] W. Kai, R. Baosen, L. Liwei, L. Yuhao, Z. Hongwei, S. Zongqiang, A review of modeling research on supercapacitor, in: Chinese Automation Congress (CAC) 2017, 2017, pp. 5998–6001, https://doi.org/10.1109/CAC.2017.8243857.
[26] A.P.R. Fernandez, E.A. Perigo, R.N. Faria, Analytical expressions for electrochemical supercapacitor with potential dependent capacitance, J. Energy Storage 43 (2021), 103156, https://doi.org/10.1016/j.est.2021.103156.
[27] P.L. Taberna, P. Simon, J.F. Fauvarque, Electrochemical characteristics and impedance spectroscopy studies of carbon-carbon supercapacitors, J. Electrochem. Soc. 150 (2003) A292.